

BMJ Open Integrating neuroimaging biomarkers into the multicentre, high-dose erythropoietin for asphyxia and encephalopathy (HEAL) trial: rationale, protocol and harmonisation

Jessica L Wisnowski ^{1,2}, Stefan Bluml,¹ Ashok Panigrahy,³ Amit M Mathur,^{4,5} Jeffrey Berman,⁶ Ping-Sun Keven Chen,⁷ James Dix,⁸ Trevor Flynn,⁹ Stanley Fricke,^{10,11} Seth D Friedman,¹² Hayden W Head,¹³ Chang Y Ho,¹⁴ Beth Kline-Fath,¹⁵ Michael Oveson,¹⁶ Richard Patterson,¹⁷ Sumit Pruthi,¹⁸ Nancy Rollins,¹⁹ Yanerys M Ramos,¹⁷ John Rampton,¹⁶ Jerome Rusin,²⁰ Dennis W Shaw,¹² Mark Smith,²⁰ Jean Tkach,¹⁵ Shreyas Vasanaawala,²¹ Arastoo Vossough,⁶ Matthew T Whitehead,¹⁰ Duan Xu,⁹ Kristen Yeom,²¹ Bryan Comstock,²² Patrick J Heagerty,²³ Sandra E Juul,²⁴ Yvonne W Wu,²⁵ Robert C McKinstry,²⁶ The HEAL Study Group

To cite: Wisnowski JL, Bluml S, Panigrahy A, *et al*. Integrating neuroimaging biomarkers into the multicentre, high-dose erythropoietin for asphyxia and encephalopathy (HEAL) trial: rationale, protocol and harmonisation. *BMJ Open* 2021;11:e043852. doi:10.1136/bmjopen-2020-043852

► Prepublication history and additional materials for this paper is available online. To view these files, please visit the journal online (<http://dx.doi.org/10.1136/bmjopen-2020-043852>).

YWW and RCM are joint senior authors.

Received 15 August 2020
Revised 11 January 2021
Accepted 31 January 2021



© Author(s) (or their employer(s)) 2021. Re-use permitted under CC BY-NC. No commercial re-use. See rights and permissions. Published by BMJ.

For numbered affiliations see end of article.

Correspondence to

Dr Jessica L Wisnowski;
wisnowsk@usc.edu

ABSTRACT

Introduction MRI and MR spectroscopy (MRS) provide early biomarkers of brain injury and treatment response in neonates with hypoxic-ischaemic encephalopathy. Still, there are challenges to incorporating neuroimaging biomarkers into multisite randomised controlled trials. In this paper, we provide the rationale for incorporating MRI and MRS biomarkers into the multisite, phase III high-dose erythropoietin for asphyxia and encephalopathy (HEAL) Trial, the MRI/S protocol and describe the strategies used for harmonisation across multiple MRI platforms.

Methods and analysis Neonates with moderate or severe encephalopathy enrolled in the multisite HEAL trial undergo MRI and MRS between 96 and 144 hours of age using standardised neuroimaging protocols. MRI and MRS data are processed centrally and used to determine a brain injury score and quantitative measures of lactate and n-acetylaspartate. Harmonisation is achieved through standardisation—thereby reducing intrasite and intersite variance, real-time quality assurance monitoring and phantom scans.

Ethics and dissemination IRB approval was obtained at each participating site and written consent obtained from parents prior to participation in HEAL. Additional oversight is provided by an National Institutes of Health-appointed data safety monitoring board and medical monitor.

Trial registration number NCT02811263; Pre-result.

INTRODUCTION

Neonatal hypoxic-ischaemic encephalopathy (HIE) is a major cause of death and neurodevelopmental disability, contributing to almost a quarter of neonatal deaths worldwide.^{1–3} Therapeutic hypothermia (TH) is

Strengths and limitations of this study

- This study will be the first to determine if high-dose erythropoietin administered to infants with moderate to severe neonatal hypoxic-ischaemic encephalopathy (HIE) reduces brain injury as measured by quantitative MRI and MR spectroscopy (MRS) biomarkers.
- MRI and MRS data are collected prospectively, using standardised MRI and MRS protocols, with quality assurance and oversight provided by the high-dose erythropoietin for asphyxia and encephalopathy neuroimaging core.
- Findings will clarify treatment effects of erythropoietin in neonates with HIE and will provide further support of efficacy.
- Limitations include the use of nine different MRI platforms and clinical workflow, which poses challenges for harmonisation and for collecting quantitative data, including MRS files. Techniques for mitigating these are discussed.

the first empirically supported therapy for neuroprotection in neonates with HIE.^{2–3} Still, even with TH, 40%–50% of neonates die or develop moderate to severe neurodevelopmental impairments.^{2,3} To improve outcomes, efforts are focused on the development and clinical translation of adjuvant neuroprotective therapies.

The high-dose erythropoietin (Epo) for asphyxia and encephalopathy (HEAL) trial (NCT02811263) is a multicentre, randomised, double-blind, placebo-controlled, phase

III clinical trial designed to test the efficacy of Epo for neuroprotection as an adjuvant to TH in neonates with moderate to severe HIE.⁴ Preclinical studies have shown that Epo induces multiple neuroprotective responses that act synergistically to reduce brain injury, promote repair and improve neurological outcomes after hypoxia-ischaemia.⁵ Recent phase I/II clinical trials support the safety of high-dose Epo and potential efficacy for neuroprotection in neonates with HIE.^{6–9} In the HEAL trial, 500 neonates with moderate or severe HIE undergoing TH will be randomised to receive Epo (1000 U/kg) or placebo on days 1, 2, 3, 4 and 7 of life. The primary endpoint is the composite of death or neurodevelopmental impairment at 24 months of age. As a secondary aim, HEAL will determine whether Epo decreases the severity of brain injury by MRI and MR spectroscopy (MRS). In this paper, we provide the rationale for incorporating MRI and MRS biomarkers into the multisite, phase III HEAL trial, the MRI/S protocol and describe the strategies used for harmonisation across multiple MRI platforms.

Neuroimaging biomarkers of neonatal HIE

Neuroimaging biomarkers provide information regarding the nature and severity of the precipitating insult, timing and prognosis. This is implied by the locus and extent of injury and the signal characteristics on T1-weighted (T1w), T2-weighted (T2w) and diffusion-weighted imaging (DWI). Additionally, advanced techniques such as MRS provide biochemical information regarding energy homeostasis and injury progression, while diffusion tensor imaging (DTI) provides information regarding microstructure and connectivity.

Patterns of injury

There are two hallmark patterns of injury associated with neonatal HIE: a central pattern involving injury to the deep grey nuclei (ventrolateral thalamus and posterior putamen) and perirolandic (paracentral) cortex, with or without concomitant injury to the brainstem and a peripheral pattern, involving injury to the white matter and/or overlying cortex in a parasagittal distribution along the vascular borderzone (watershed territory). These patterns are similar to the patterns of injury observed experimentally in primates following 'near total' and 'prolonged partial' asphyxia, respectively.^{10–14} Other commonly observed findings in neonates with HIE include punctate white matter lesions, focal lesions (including strokes) and haemorrhages (intraventricular, intraparenchymal and extra-axial), as well as 'normal' MRIs (no apparent injury).^{15–20}

Epidemiological neuroimaging data are limited, and thus, the prevalence of various injury patterns in neonates with mild, moderate or severe HIE, as classified by Sarnat Stage, is not known. Multiple studies have investigated whether the pattern of injury varies by maternal–fetal factors, including sentinel events during delivery and placental function; however, a consistent pattern has yet to emerge. Several studies have shown that sentinel

events were associated with an increased risk of injury to the thalamus/basal ganglia and/or cortex and white matter^{21 22}; however, the opposite has also been found.²³ Likewise, placental abnormalities have been associated with HIE^{24–26}; however, there has been inconsistency with regard to which placental findings are associated with which pattern(s) of injury.^{27–30}

Timing and evolution of HIE brain injury

HIE injury evolves over days, and serial imaging has demonstrated this evolution is associated with varying signal abnormalities on T1w and T2w MRI, DWI and MRS. Acutely, injury appears as areas of restricted diffusion on Trace-DWI and apparent diffusion coefficient (ADC) maps. Quantitative measurements obtained in neonates with HIE show that ADC values reach their nadir 2–3 days after birth and rise thereafter, pseudonormalising at approximately 1 week after birth.^{31 32} These curves are similar at 1.5 and 3T; however, measured ADC values are inversely related to b-value, and higher b-values ($\geq 1000 \text{ s/mm}^2$) are more sensitive for detecting acute injury.^{33 34} TH augments the ADC curve producing lower ADC values and may extend the time window for pseudonormalisation to as late as 8–10 days of age.³⁵

Conventional MRI demonstrates parallel signal changes. Acutely, oedema appears as areas of low signal and high signal on T1w and T2w MRI, respectively. These areas may show corresponding low ADC values indicating cytotoxic oedema (cell swelling). As injury evolves, focal areas of T1 hyperintensity with correspondent T2 hypointensity begin to appear in the deep grey and/or cerebral cortex, especially, in the ventrolateral thalamus, posterolateral putamen and perirolandic cortex. Additionally, T1w and T2w imaging may show disruption of the normal cortical ribbon, particularly in borderzone (watershed) regions or in the vicinity of other focal injuries (eg, infarcts, contusions).

MRS demonstrates comparable changes in metabolite concentrations during the first and second week after birth. Acutely, there is a rise in lactate, a marker of anaerobic metabolism; however, lactate peaks during the first week, followed by a rise in lipids, which are only detectable at short echo time.³⁶ By contrast, n-acetylaspartate (NAA), a marker of neuronal mitochondrial metabolism, declines during the first few days and then remains lower among HIE infants with brain injury.^{32 37–39} Other metabolites show transient changes following HIE including phosphocreatine, myoinositol, glutamine and choline.^{40–43}

In conjunction with evolving signal abnormalities on T1w, T2w, DWI and MRS, serial imaging has also shown that the locus of injury may evolve during the first week. This is especially common among infants with injury to the deep grey matter who often demonstrate injury localised to the ventrolateral thalamus + dorsal brainstem on early scans (1–3 days of age), followed by more widespread injury in the deep grey nuclei (particularly posterolateral putamen) and perirolandic cortex on later

scans (4+ days).^{15 32 44} Moreover, as injury evolves, areas of Wallerian degeneration often appear on DWI, including in the posterior limb of the internal capsule (PLIC), splenium and brainstem.^{15 32}

MRI as a prognostic biomarker

MRI is widely employed clinically as a prognostic biomarker, and several semiquantitative scoring systems have been developed for use in clinical research.^{16 17 20 45–49} Most of these systems place greater weight on injury to the grey matter (thalamus, basal ganglia and perirolandic cortex) as these findings have been most consistently associated with adverse outcomes, including death and neurodevelopmental impairment.^{16 20 45–49} However, scoring systems differ with regard to how they quantify severity, with some inferring severity from the locus of the injury alone^{16 39 45} while others infer severity from the locus and extent of signal abnormality.^{20 48} Several yield information regarding pattern of injury.^{16 44 45} None provide quantitative information regarding stage (ie, acute, subacute, chronic) based on the evolving signal abnormalities on MRI.

Several studies have assessed the validity of the semiquantitative MRI scores in single centre^{45 48} and multicentre studies.^{16 20 39 47 50 51} These studies have demonstrated variable accuracy for predicting death or neurodevelopmental impairment at follow-up, ranging from area under the curve (AUC) 0.7–0.99.^{20 37 48 51} Some of this variability in predictive accuracy may be accounted for by the timing of the MRI exams and the sequences employed. Several studies have suggested that early scans (<1 week) may provide better sensitivity while later scans provide better specificity.^{51 52}

Multiple studies have shown that MRS enhances the predictive accuracy of MRI^{20 37 51} and several studies have suggested that MRS may provide the highest predictive accuracy of all MRI biomarkers.^{39 51} By contrast, quantitative ADC measurements have poor prognostic accuracy,⁵¹ likely due to pseudonormalisation, as discussed above.

Neuroimaging biomarkers in prior randomised controlled trials for neuroprotection

MRI was included as a secondary outcome in three previous phase III randomised controlled trials (RCTs) for TH: the NICHD Neonatal Research Network (NRN) Trial (2005),¹⁶ the Total Body Hypothermia for Neonatal Encephalopathy (TOBY) Trial (2009)¹⁷ and the Infant Cooling Evaluation (ICE) Trial (2011).⁴⁷ All three trials found that TH was associated with less injury on MRI. Furthermore, the sensitivity and specificity of the MRI biomarkers for predicting adverse outcome did not differ between neonates who received TH and those who received normothermia (NT), indicating that TH did not alter the prognostic value of MRI in neonates with HIE.

However, the MRI results from the three cooling trials varied in several important aspects. First, although TH was associated with less brain injury on MRI in each trial, the nature of the effect varied. In the TOBY Trial, TH

was associated with a reduction in signal abnormalities in the basal ganglia/thalamus (BGT) (OR 0.36, 95% CI 0.15 to 0.84; $p=0.02$), white matter (0.30, 0.12 to 0.77; $p=0.01$), and PLIC (0.38, 0.17 to 0.85; $p=0.02$).¹⁷ In contrast, TH was not associated with a significant reduction in BGT injury in either the NICHD NRN or ICE trial, but was associated with a significant reduction in injury to the cortex and underlying white matter.^{16 47}

The inconsistent MRI findings in the three cooling trials are likely due, at least in part, to differences in study design, including inclusion criteria, cooling technology and neuroimaging methods. Moreover, only a subset of patients in each trial had analyzable MRI data, and both the proportion of patients in the MRI subanalyses, which ranged from 40% to 65%, and relative proportion assigned to each treatment group (TH vs NT) varied across trials.^{16 17 47} Likewise, the MRI protocols differed between trials (e.g., with or without DWI) as did the timing of imaging, with mean age ranging from 6⁴⁷ to 15 days.¹⁶ Consistent with the variability in the neuroimaging methods, the sensitivity and specificity of MRI biomarkers as predictors of outcome varied substantially across trials, with the highest sensitivity—but low specificity—in the NICHD NRN trial, and the highest specificity—but low sensitivity—in ICE.^{16 17 47} This variability limits any conclusions regarding differences in neuroimaging outcomes across the three TH trials and points to the necessity of standardisation and harmonisation.

Special considerations for MRS

Incorporating MRS into multisite trials poses additional challenges beyond those encountered for conventional MRI. Many hospitals do not routinely acquire MRS in neonates with HIE as MRS requires specific software packages, which may not have been purchased. MRS acquisition is also more technically demanding due to its low signal to noise ratio (SNR) compared with conventional MRI.⁵³ There are also challenges associated with detection of lactate and other j-coupled metabolites that must be addressed at acquisition and/or postprocessing in order to avoid known pitfalls.⁵⁴ Likewise, MRS analysis and interpretation are more complex than conventional MRI and require expert knowledge beyond core competence in diagnostic radiology. Last, MRS has its own separate billing code, and reimbursement is poor, often requiring preauthorisation. Thus, although recommended by the American College of Obstetrics and Gynecology task force on Neonatal Encephalopathy and endorsed by the American Academy of Pediatrics for assessment of brain injury in neonatal HIE,⁵⁵ MRS usage lags behind MRI.

MRS was not systematically incorporated into any prior multicentre, phase III cooling trials for HIE, but it has been incorporated into single-centre^{32 41–43 56–58} and multicentre observational studies^{39 59} as well as several recent phase I/II RCTs.^{60 61} The sensitivity and specificity of MRS for predicting outcome is not affected by TH, making it suitable for use as a prognostic biomarker in neonates undergoing TH for HIE.^{39 51 57 62–64} As with MRI,

the reliability and diagnostic accuracy of MRS biomarkers may be affected by the timing of exam, sequence parameters (short echo vs long echo), region sampled (BGT vs white matter), postprocessing methods (ratios vs absolute quantitation) and the precise metabolites chosen (eg, lactate, NAA, creatine, choline).^{39 51 52}

METHODS

In this section, we present the HEAL Neuroimaging Protocol in accordance with the Standard Protocol Items: Recommendations for Interventional Trials (SPIRIT) reporting guidelines.⁶⁵

Study design

The HEAL trial is a multicentre, phase III, randomised, double-blind, placebo-controlled trial involving 500 neonates, ≥ 36 weeks gestational age with moderate to severe HIE who are undergoing TH. Treatment allocation (Epo or placebo) is parallel (1:1), stratified by site and HIE severity. Parents, participants and study personnel—including the Neuroimaging Core—are blinded to the treatment group. For further details regarding the HEAL trial, please see online supplemental appendix 1 and also Juul et al.⁴

MRI and MRS data are obtained at 4–5 days of age as part of routine clinical care, using a standardised MRI protocol. Neuroimaging data are then analysed centrally by the HEAL Neuroimaging Core. Details regarding acquisition, data transfer, data processing and analyses are provided in the next section.

Patient and public involvement

This study was designed by the HEAL Study Group. There is no parental advisory board. Results will be disseminated to other physicians via academic medical conferences and to the public at large via standard press releases.

Study locations

The HEAL trial is being carried out across a network of 17 study sites, using 9 MR platforms (table 1). Five of the sites include two or more enrolling hospitals. Each of the participating hospitals has a 3T MR system, with the exception of one hospital, which is using a 1.5T MR system and a dedicated neonatal head coil.

MRI and MRS sequences and sequence parameters

Prior to the start of HEAL enrolment, detailed MRI protocols were developed for each MRI platform. During the preparatory phase, we compared different sequences and sequence parameters across platforms in order to maximise consistency in image contrast, resolution and SNR across platforms using US Food and Drug Administration-approved product sequences. The final protocol is presented in table 2 (see also figures 1 and 2, eg, images). One limitation is that we were not able to find an optimal solution for a 3 dimensions (3D) T2w sequence. Therefore, we used a 2D sequence, with the in-plane resolution matched to our 3D T1w sequence and

slice thickness at 2 mm (no gap) in alignment with our DTI sequence.

The MRS protocol includes both short echo (TE 35) and long-echo (TE 288) acquisitions. Furthermore, the decision to use TE 288 over TE 144 mitigates a known pitfall with lactate at 3T, namely the attenuation and even absence of signal at TE 144 due to anomalous j-coupling,⁵⁴ while the short echo (TE 35) acquisitions allow for quantitation of additional metabolites, including glutamate, glutamine and lipids.

Timing of brain MRI and MRS

The target window for the HEAL MRI is day 4 or 5 after birth (between 96 and 144 hours of age). This window corresponds to a period of maximal sensitivity and specificity for MRI and MRS⁵¹ when abnormal DWI/ADC signal is maximised^{51 57} and risk of pseudonormalisation is minimised.^{31 44} Furthermore, this timing is compatible with current clinical practice and provides information to guide medical management including decisions about redirection of care. For those infants who are not clinically stable for MRI during this window, MRIs are obtained as soon after the infant becomes clinically stable as possible.

Use of sedation

Because HEAL MRI scans are performed as part of routine clinical care, the use of sedation is determined locally by the attending physicians on a case-by-case basis. Given concerns regarding possible neurotoxic effects of anaesthetic drugs,⁶⁶ every effort has been made to facilitate non-sedated imaging whenever possible. To determine whether sedatives affect MRS metabolite concentrations, all psychoactive medications administered within 4 hours of the examination are recorded in the HEAL database.

Anonymisation and data transfer

Anonymisation and transfer of neuroimaging data is facilitated by using a secure, Health Information Portability and Accountability Act (HIPAA)-compliant, cloud-based service (Ambra Health, New York, New York, USA). Because raw quantitative MRS data are not compatible with clinical PACS systems, we developed specific protocols to transfer these data from the MR scanner in standard DICOM (Siemens), enhanced DICOM (Philips), P-files (GE) other file formats (eg, SPAR/SDAT, RDA), as needed. Furthermore, although the cloud-based service provides anonymisation on upload to the HEAL Neuroimaging Core, uploading the raw MRS data requires anonymisation prior to or during export from the MR scanner as detailed in table 3.

Data processing: MRI

The primary HEAL neuroimaging outcome measures is the total MRI injury score based on a previously validated MRI scoring system for HIE.⁴⁸ This score indicates the extent of signal abnormality (ie, 0=none, 1 $\leq 25\%$, 2=25%–50%, 3 $\geq 50\%$) for each of the deep grey nuclei, PLIC, cerebral cortex, white matter and cerebellum, as well as brainstem (scored on a 0–2 scale) separately for

Table 1 Participating sites

Site	Hospital	MR manufacturer	Model	Software	On-site support for HEAL
Seattle, WA*†‡	Seattle Children's Hospital	Siemens	Prisma	E11	Physicist
Columbus, OH	Nationwide Children's Hospital	Siemens	Skyra	E11	Physicist
Dallas, TX	Parkland Hospital	Siemens	Skyra	E11	MR Technologist
Indianapolis, IN	Riley Hospital for Children	Siemens	Skyra	E11	MR Technologist
Minneapolis-St. Paul, MN‡	Children's Hospital and Clinics of Minnesota: Minneapolis	Siemens	Skyra	E11	MR Technologist
Minneapolis-St. Paul, MN‡	Children's Hospital and Clinics of Minnesota: St. Paul	Siemens	Skyra	E11	MR Technologist
Philadelphia, PA	Children's Hospital of Philadelphia	Siemens	Skyra	E11	Physicist
Pittsburgh, PA‡§	Children's Hospital of Pittsburgh of UPMC	Siemens	Skyra	E11	Physicist
Fort Worth, TX	Cook Children's Medical Center	Siemens	Verio	B19	MR Technologist
San Antonio, TX‡	Children's Hospital of San Antonio	Siemens	Verio	D13	MR Technologist
San Antonio, TX‡	Methodist Children's Hospital	Siemens	Trio	B17	MR Technologist
St. Louis, MO§	Washington University Medical Center/ St. Louis Children's Hospital	Siemens	Trio	B17	Physicist
Nashville, TN	Vanderbilt University Medical Center	Philips	Achieva	3.2	MR Technologist
Seattle, WA*, †‡	University of Washington Medical Center	Philips	Achieva	5.3	Physicist
Cincinnati, OH	Cincinnati Children's Hospital Medical Center	Philips	Ingenia	5.3	Physicist
Los Angeles, CA§	Children's Hospital Los Angeles	Philips	Ingenia	5.1.7	Physicist
San Francisco, CA*§	UCSF Benioff Children's Hospital	GE	750	DV25	Physicist
Stanford, CA	Stanford University Medical Center	GE	750	DV26	Physicist
Washington, DC	Children's National Medical Center	GE	750	DV26	Physicist
Salt Lake City, UT	Primary Children's Medical Center/Univ. of Utah	GE	Architect	DV27	MR Technologist
Pittsburgh, PA‡	UPMC Magee Women's Hospital	GE	HDx [¶]	DV24	Physicist

*Clinical Coordinating Centre.

†Data Coordinating Centre.

‡Denotes sites with more than one enrolling hospital.

§Neuroimaging core.

¶1.5T MR system with dedicated neonatal head coil.

HEAL, high-dose erythropoietin for asphyxia and encephalopathy.

each sequence as shown in [table 4](#). 'Signal abnormality' is defined qualitatively as either abnormally low or high signal on T1w and T2w images or areas of restricted diffusion on Trace-weighted or ADC images calculated from the DTI sequence. We do not employ a quantitative threshold for ADC, consistent with the previously validated scoring system.^{7 48} Areas with high ADC are not scored as injury for the DTI images, which is designed to measure acute injury; however, correspondent areas of low and/or high signal on the T1w and/or T2w images are scored.

For each ROI, injury is scored qualitatively for each sequence on a 4-point scale based on the extent of signal abnormality (0=none, 1 = <25%, 2=25%–50%, 3 ≥50%),

except for the brainstem which is scored on a 3-point scale (0=none; 1=focal; 2=multifocal/widespread).

To compute the MRI injury score, each scan is reviewed independently by two of three experienced readers (AMM, JLW and RCM), who are blinded to the infant's clinical course, treatment assignment and MRS findings. After the primary review, each scan undergoes final consensus review during which any discrepancies are reviewed by all three reviewers and resolved by consensus. The individual and consensus scores are then classified as none (total=0), mild (1–11), moderate (12–32) or severe (33–138), in accordance with the previously validated MRI injury classification.⁴⁸ Inter-rater reliability between the three independent readers will be determined for

**Table 2** HEAL MRI sequences and sequence parameters

	Siemens (Prisma, Skyra, Verio, Trio)	Philips (Achieva, Ingenia)	GE (MR750, MR750w, Architect)
T1w (3D)			
Sequence	MPRAGE	3D-TFE	IR-SPGR
Resolution	1×1×1 mm	1×1×1 mm	1×1×1 mm
Slice orientation	Sagittal	Sagittal	Sagittal
TI	1100 ms	1000 ms	700 ms
TE	3.05 ms	4.6 ms	3.16 ms
TR	1550 ms	9.9 ms	8.15 ms
Flip Angle	15	8	12
Echo spacing*	9 ms	9.9 ms	8.36 ms
Shot interval*	1550 ms	2000 ms	10.5 ms
Bandwidth (pixel)	130 Hz	149 Hz	163 Hz
Acceleration	GRAPPA (none)	SENSE (none)	SENSE (none)
Reformats	Axial, Coronal	Axial, Coronal	Axial, Coronal
TA	3:45	4:13	4:00
T2w (2D)			
Sequence	TSE or BLADE	TSE or MULTIVANE	FSE or PROPELLER
Resolution	1×1×2 mm	1×1×2 mm	1×1×2 mm
TE	≥120 ms (target=160 ms)	≥120 ms (target=160 ms)	≥120 ms (target=160 ms)
TR	10000 ms	10000 ms	≥7000 ms
ETL	15	15	13
Acceleration	GRAPPA=2	SENSE=1.3	ASSET (≤2)
TA	3:02	3:20	3:30
DTI			
Sequence	Ep_2D	DTI ('High')	DTI (30-dir)
Resolution	2×2×2 mm	2×2×2 mm	2×2×2 mm
TE	81 ms	88 ms	88 ms
TR	10200 ms	10000 ms	7500 ms
No of Dir.	30	32	30
Max b-value	1000 s/mm ²	1000 s/mm ²	1000 s/mm ²
Acceleration	GRAPPA (2)	SENSE (2.2)	SENSE (2.2)
TA	4:49	5:18	5:00
MRS			
Sequence	SVS-SE	PRESS	PROBE
Resolution	17×17×17 (Thal/BG) 15×15×15 (par. WM)	17×17×17 (Thal/BG) 15×15×15 (par. WM)	17×17×17 (Thal/BG) 15×15×15 (par. WM)
TE	35 ms (short-echo) 288 ms (long-echo)	35 ms (short-echo) 288 ms (long-echo)	35 ms (short-echo) 288 ms (long-echo)
TR	2000 ms	2000 ms	2000 ms
Bandwidth	2000 Hz	2000 Hz	2000 Hz
NSA (metabolite)	128	128	128
NSA (water)	6	16	16
TA	4:28	4:48	4:48

*Note that although all three vendors use an ultrafast gradient echo sequence, the IR-SPGR (GE) differs from the others with regard to the timing of the gradient echoes during acquisition, which prohibits direct comparisons between echo spacing and shot intervals across vendors.

3D, 3 dimensions; DTI, diffusion tensor imaging; ETL, echo train length; FSE, fast spin echo; GRAPPA, Generalized Autocalibrating Partially Parallel Acquisition; HEAL, high-dose erythropoietin for asphyxia and encephalopathy; IR-SPGR, Inversion prepped spoiled gradient echo sequence; NSA, Number of signal averages; SENSE, SENSitivity Encoding; TA, acquisition time; TE, echo time; TFE, Turbo Field Echo; TR, repetition time; TSE, turbo spin echo; T2W, T2 weighted.

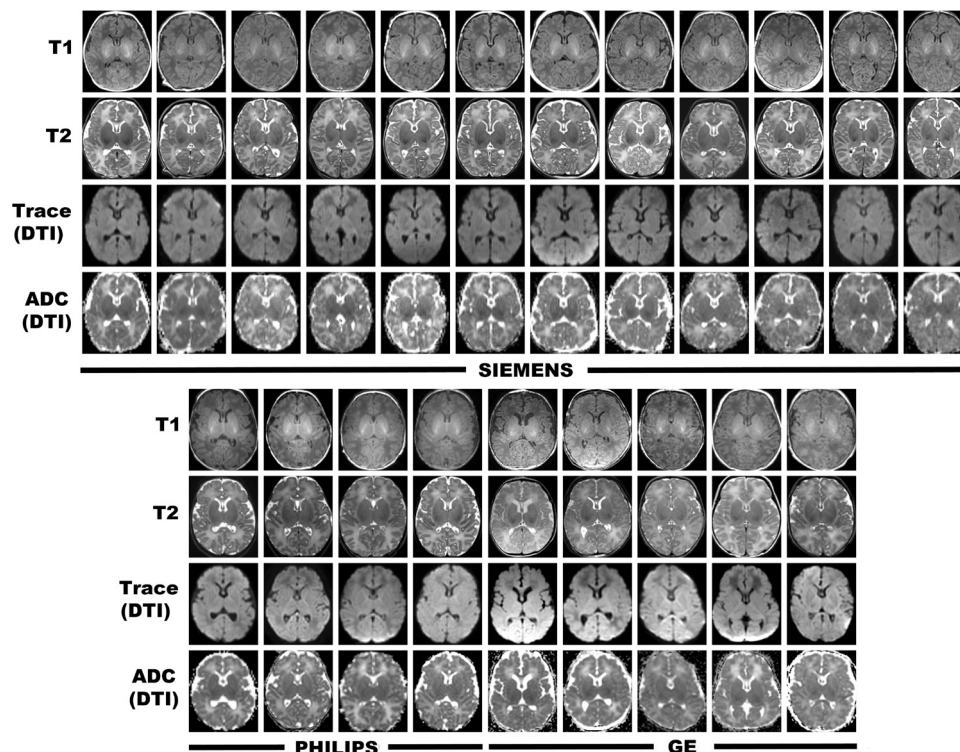


Figure 1 Representative HEAL MRI at the level of the PLIC obtained at each of the participating HEAL sites. Harmonisation centred on ensuring consistent sequences, sequence parameters and image resolution within and across participating sites. ADC, apparent diffusion coefficient; DTI, diffusion tensor imaging; HEAL, High-Dose Erythropoietin for Asphyxia and Encephalopathy.

both the total score and for the categorical classification (none, mild, moderate, severe). For the total score, we will use a general linear mixed effects model to estimate the intraclass correlation coefficient (ICC).⁶⁷ For the categorical classification, we will use kappa.⁶⁸ Secondary MRI measures include the MRI injury severity classification discussed above as well as classification of injury pattern and acuity. Injury pattern is classified as: (1) normal MRI (defined as no evidence of injury); (2) central (injury to

the BGT±perirolandic cortex); (3) peripheral (injury to the parasagittal cortex and/or WM, ie, 'borderzone/water-shed distribution'); (4) global (injury to BGT+ total or near total involvement of cortex±underlying WM); (5) punctate WM Lesions (discrete foci of injury typically 1–10 mm in size localised to the periventricular WM or centrum semiovale); (6) arterial ischaemic stroke (infarct localised to the vascular territory of the middle, anterior or posterior cerebral arteries); (7) other focal lesions (includes

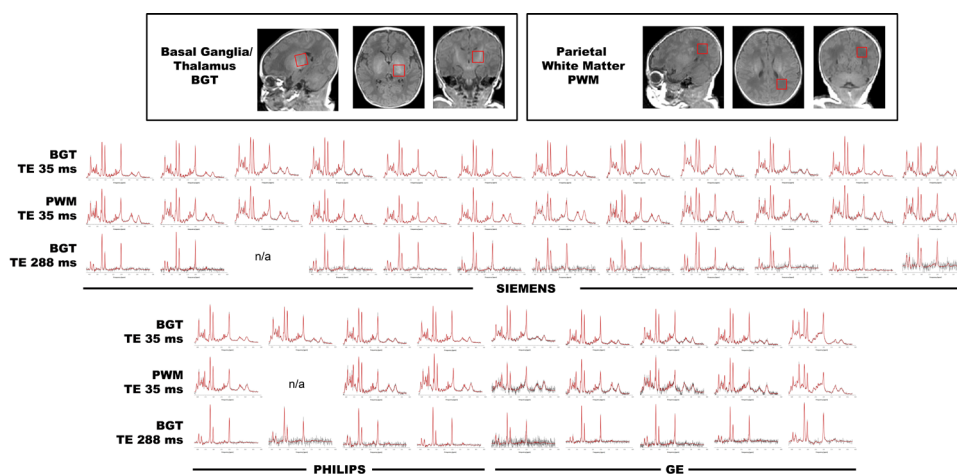


Figure 2 Representative MR spectra acquired at each of the participating HEAL sites on the same patients as in figure 1. Note that two spectra were not available (n/a) from two patients above due to site-specific protocol constraints (top row) and a technical problem (bottom row). HEAL, high-dose erythropoietin for asphyxia and encephalopathy; n/a, not available; TE, echo time.

Table 3 Procedures for exporting raw MRS data

	Siemens	Philips	GE
Standard DICOM format	IMA	Enhanced DICOM Classic DICOM	n/a
Non-DICOM format	RDA	SPAR/SDAT	P-file (Pxxxxx.7)
Preferred format for export	IMA	Enhanced DICOM	P-file (Pxxxxx.7)
Anonymisation	During DICOM export	During DICOM export	Prior to export by way of <i>pfile_anon</i> (GE software)
Limitations	Requires direct export to flash drive. If exporting to CD/DVD, anonymisation must be done manually	If scanner not configured to export enhanced DICOM, it may be necessary to export SPAR/SDAT, followed by manual anonymisation of SPAR file	If scanner not configured to allow for telnet access, P-file must be exported to DVD followed by manual anonymisation of P-file

CD, compact disc; DICOM, Digital Imaging and Communications in Medicine, which is the international standard to transmit, store, retrieve, print, process, and display medical imaging information; DVD, digital versatile disc.

venous infarcts, contusions, and unilateral lesions to the BGT, cortex or white matter not classified elsewhere) and (8) atypical/not otherwise specified (with additional text field for describing the lesion). The scoring system allows for multiple patterns to be coded, which will allow us to determine the frequency of individual patterns as well as the co-occurrence across patterns.

Acuity is defined by the co-occurrence of signal abnormalities across the MRI sequences. Of note, the HEAL MRI examination occurs on day 4 or 5, prior to the expected pseudonormalisation of the ADC signal, and final analyses will be restricted to patients whose MRIs were completed within the first week. Acute lesions are defined as lesions

that show correspondent diffusion restriction. Subacute lesions are defined as lesions (signal abnormalities) on T1w and/or T2w images without correspondent diffusion restriction (high or 'normal' ADC signal). Chronic lesions are defined as lesions associated with volume loss and tissue remodelling (eg, porencephalic cysts). As for injury pattern, the scoring system permits coding multiple levels of acuity (eg, acute + subacute injury).

Data processing: MRS

The primary MRS outcome measure is the ratio of lactate to NAA. As secondary analyses, we will also determine lactate and NAA concentrations (mmol/kg) as well as

Table 4 HEAL/Wash U MRI scoring system

	T1	T2	Trace/ ADC	BGT subscore	Total score
Caudate					
Putamen/GP					
Thalamus					
PLIC					
Cortex					
White Matter					
Brainstem					
Cerebellum					
Injury pattern(s):	<ul style="list-style-type: none"> ▶ Normal MRI (no evidence of injury) ▶ Central HIE Pattern (BGT±periolentic cortex) ▶ Peripheral Pattern (Parasagittal cortex and/or WM, that is, 'watershed') ▶ Global Injury Pattern (BGT +total or near total involvement of cortex/WM) ▶ Punctate WM Lesions (discrete foci of injury (typically ~1 to 10 mm in size localised to the periventricular WM or centrum semiovale) ▶ Arterial Ischaemic Stroke ▶ Other focal lesion (includes venous infarct±IPH; contusion; unilateral lesions in BGT or other GM/WM not classified elsewhere) ▶ Atypical pattern (please specify: 			Classification (independent of the scores above)	

ADC, apparent diffusion coefficient; BGT, basal ganglia/thalamus; HEAL, high-dose erythropoietin for asphyxia and encephalopathy; HIE, hypoxic-ischaemic encephalopathy.

additional MRS metabolites. Raw MRS data (ie, quantitative files, see [table 3](#)) are processed centrally under the direct supervision of SB and JLW using a modified LCModel (V6.3–1L, Stephen Provencher, Oakville, Ontario, Canada) pipeline. This fully automated pipeline applies zero-order and first-order corrections for phase, estimates a baseline, corrects for ppm shift and eddy currents, and determines metabolite concentrations, all without need for user interaction. Data are fitted with linear combinations of model spectra of known concentration from a standard basis set. For quantitation, the unsuppressed water signal is used as a concentration reference, with tissue water content estimated at a standardised value (ie, 86% or 47.8M) consistent with prior published methods.^{43 69}

Statistical analyses

The primary neuroimaging outcome measures are: (1) the total injury score (derived from the HEAL/Wash U MRI scoring system above) and (2) the ratio of lactate/NAA determined for the left thalamus and parietal white matter from the quantitative MRS data. For the MRI injury score and the lactate/NAA ratio, we will use linear regression to compare Epo treated patients to controls while adjusting for site and HIE severity since these are factors used to stratify the randomisation. In the event that we have missing data due to either early patient death or other factors (eg, family declines MRI or infant is unable to complete all of the sequences), we will estimate the resultant sampling bias by comparing our final neuroimaging sample to the overall HEAL sample with regard to patient demographics and primary outcome data.

Sample size

The sample size for the HEAL trial (n=500) is designed to yield greater than 90% power to detect a relative reduction in the rate of death or neurodevelopmental impairment (primary outcome) of 33% in the Epo group as compared placebo group.⁴ To calculate the sample size necessary for the secondary neuroimaging analyses, we first calculated the observed effect size for the MRI injury score for the prior phase II trial.⁷ This study demonstrated a lower brain injury score in Epo-treated infants as compared with placebo (mean 5.26±9.9 vs 16.36±18.3, p<0.01, Cohen's d=0.75) and a lower rate of moderate/severe brain injury (4% vs 44%, p<0.002). Using a conservative effect size for HEAL (Cohen's d=0.75/2) and controlling for multiple comparisons, a total sample size of 356 will yield greater than 90% power to detect a medium size effect (Cohen's d=0.375) on brain injury as measured by the MRI injury score or lactate/NAA biomarker.

Neuroimaging harmonisation and quality assurance

The primary goal of harmonisation is to reduce measurement error by maximising the consistency of neuroimaging data within and across sites. Minimising measurement error maximises the standardised effect size and therefore statistical power.⁷⁰ Intrasite and intersite variability in

MRI measurements can arise due to variability in: (1) MR hardware (eg, field strength, gradient strength, sensitivity of the head coils, hardware upgrades); (2) software (eg, sequences, sequence parameters, software upgrades); (3) patient workflow (eg, whether an infant is sedated or fed/swaddled in an infant immobiliser; whether the infant is properly positioned in the centre of the head coil) and (4) the timing of the MRI (eg, before or after expected pseudonormalisation of the diffusion signal). Additionally, noncompliance, a common challenge in multisite studies, contributes further error. Although it is possible to include 'site' as a covariate in statistical models, site and scanner effects are often non-linear and non-uniform across the brain as well as sequence-specific, making them challenging to manage retrospectively using statistical techniques. Accordingly, managing harmonisation prospectively through study design and real-time monitoring are key to ensuring the reliability and reproducibility of the neuroimaging biomarkers.

Our harmonisation efforts for HEAL centre on two areas: (1) a certification process to ensure that each site was able to obtain high-quality data in accordance with the HEAL protocol and (2) a robust quality assurance process designed to monitor acquisition and mitigate errors in a timely fashion throughout the trial. Prior to the start of HEAL, we developed a standardised MRI/S protocol and verified that it could be carried out across platforms to generate resultant images that were comparable across platforms with regards to tissue contrast, resolution and SNR. Because the HEAL MRIs are acquired as part of standard clinical care, as part of site initiation, we had discussions with at least one neuroradiologist from each site, as well as site PI, to ensure that the proposed HEAL MRI/S protocol would meet the site's requirements for a clinical MRI protocol and to mitigate any site-specific challenges implementing the HEAL protocol. Additionally, each site provided a test dataset, which were used to verify sequence parameters, image homogeneity, slice orientation and motion. MRS data were reviewed for voxel position and raw data was processed to ensure adequate line width and SNR. Furthermore, the test scans certified the data transfer process and ensured that all data, including raw MRS, could be captured from each site and transferred to the HEAL Neuroimaging Core.

During the enrolment period, quality assurance is maintained through a real-time process aimed at monitoring acquisition and mitigating any protocol deviations. All brain MRI and MRS data are reviewed shortly after being uploaded to the HEAL database. Any protocol deviations are recorded and each sequence (T1w, T2w and DTI) is scored for motion on a four-point scale: none, mild (unlikely to affect interpretation), moderate (may affect interpretation), severe (obscures interpretation). Likewise, MRS sequence parameters and voxel positions are reviewed, and raw data are checked to ensure that valid files are present for MRS processing. All protocol deviations and severe motion or other artefacts are immediately discussed with the site.



Phantom studies

The primary HEAL MRI and MRS endpoints, namely the total MRI injury score and the ratio of lactate/NAA, were designed to be robust across a wide range of scanner platforms. However, to take full advantage of potential secondary analyses, including quantitative MRS and DTI biomarkers, we are carrying out additional phantom studies during the HEAL trial. These phantom studies are aimed at further reducing unwanted site-related and scanner-related variance from our quantitative MRS and DTI measures. For MRS, we are using a commercially available phantom (GE Healthcare), which contains physiological concentrations of NAA, lactate, creatine, choline, glutamate and myoinositol. For DTI, we are using the diffusion ice-water phantom, which leverages the known properties of water diffusion at 0°C.⁷¹ Both phantoms will be scanned on multiple days at the HEAL neuroimaging core and twice within a single session at participating HEAL sites using the HEAL MRS and DTI protocols. We will use these data to compute the coefficient of variation for each metabolite concentration and ADC value across MR vendors, platforms and sites. These data will not only provide an estimate of the degree of measurement error that is attributable to scanner and site-specific effects, but also help to inform whether we will need to deploy additional retrospective statistical approaches (eg, ComBat⁷²) to address unwanted site-related and scanner-related variance.

Unfortunately, we could not identify comparable phantoms with appropriate T1 and T2 values for an infant brain and employing a ‘travelling infant’ as a phantom was impractical. Thus, further harmonisation of the T1w and T2w data will have to be carried out using retrospective statistical approaches.

DISCUSSION

The search for new neuroprotective therapies is ongoing, not only for neonatal HIE, but also a range of disorders, including stroke, traumatic brain injury and cardiac arrest. As preclinical studies identify promising therapies, the research community needs reliable biomarkers with which to move promising therapies from phase II to phase III trials. This is critical, given the scarce resource of appropriate patients and the cost of clinical trials. Neuroimaging biomarkers can help facilitate clinical translation by providing early endpoints for evaluating treatment efficacy. Furthermore, they can be used to elucidate treatment effects and the mechanisms by which improvements in neurological outcomes are achieved.

At the same time, ensuring the reliability and reproducibility of neuroimaging data across a large-scale, multisite RCT remains challenging. As a field, some of these challenges could be mitigated by adopting common protocols for neuroimaging. This would not only aid in the reproducibility within and across trials, but also strengthen research from bench to bedside by providing a means for directly comparing the effects of therapies in preclinical and clinical trials to those obtained in clinical practice. Last, some of the technological challenges, such as MRS

data transfer and storage, would be eliminated if manufacturers were to use the standard DICOM format for archiving MRS data, as was done for conventional MRI more than three decades ago.

Summary

HEAL is the first phase III RCT for neuroprotection to incorporate MRI, DTI and MRS biomarkers on a large scale. We present standardised MRI and MRS protocols for HIE that are feasible on any modern 3T platform and describe our rigorous quality assurance procedures. Using phantom studies, we will characterise the degree of unwanted site-specific and scanner-specific effects remaining after harmonisation, which, in turn, will be used to estimate the need for advanced statistical methods to reduce such nuisance variance. Together, these methods will ensure rigour and reliability of the neuroimaging biomarkers collected in the HEAL trial and may help inform the design of future neonatal neuroprotection trials.

ETHICS AND DISSEMINATION

The study protocol (currently: V.2.9, 18 March 2020), site-specific informed consent forms, participant education and recruitment materials and all study modifications have been approved by the local Institutional Review Board at each of the participating sites. Parents have provided written permission for their child’s participation in the HEAL trial. Safety and progress reports are provided to the NIH-appointed data safety monitoring committee every 6 months.

Study findings will be disseminated through scientific conferences, peer-reviewed journal publications, public study website materials and invited lectures. Results from this study will be reported according to SPIRIT guidelines⁶⁵ and submitted for peer-reviewed publication. Individual participant data, including neuroimaging data, will be made available through the National Institute of Neurological Disorders and Stroke (NINDS) Data Archive: <https://www.ninds.nih.gov/Current-Research/Research-Funded-NINDS/Clinical-Research/Archived-Clinical-Research-Datasets>. The data will be deidentified and a limited access data set will be available after March 2024 through a request form on that page. Data dictionaries, in addition to study protocol, the statistical analysis plan and the informed consent form will be included.

Author affiliations

¹Radiology, Children’s Hospital of Los Angeles, Los Angeles, California, USA

²Pediatrics, Children’s Hospital Los Angeles Division of Neonatology, Los Angeles, California, USA

³Radiology, Children’s Hospital of Pittsburgh of University of Pittsburgh Medical Center, Pittsburgh, Pennsylvania, USA

⁴Pediatrics, Division of Neonatal-Perinatal Medicine, SSM Health Cardinal Glennon Children’s Hospital, Saint Louis, Missouri, USA

⁵Pediatrics, Division of Neonatal-Perinatal Medicine, Saint Louis University, Saint Louis, Missouri, USA

⁶Radiology, The Children’s Hospital of Philadelphia, Philadelphia, Pennsylvania, USA

⁷Radiology, Children’s Hospital of San Antonio, San Antonio, Texas, USA

⁸Radiology, Methodist Children’s Hospital, San Antonio, Texas, USA

- ⁹Radiology, University of California San Francisco, San Francisco, California, USA
¹⁰Radiology, Children's National Medical Center, Washington, District of Columbia, USA
¹¹Radiology, Georgetown University Medical Center, Washington, District of Columbia, USA
¹²Radiology, Seattle Children's Hospital, Seattle, Washington, USA
¹³Radiology, Cook Children's Medical Center, Fort Worth, Texas, USA
¹⁴Radiology, Indiana University School of Medicine, Indianapolis, Indiana, USA
¹⁵Radiology, Cincinnati Children's Hospital Medical Center, Cincinnati, Ohio, USA
¹⁶Radiology, Primary Children's Hospital, Salt Lake City, Utah, USA
¹⁷Radiology, Children's Hospitals and Clinics of Minnesota, Minneapolis, Minnesota, USA
¹⁸Radiology, Vanderbilt University, Nashville, Tennessee, USA
¹⁹Radiology, University of Texas Southwestern Medical School, Dallas, Texas, USA
²⁰Radiology, Nationwide Children's Hospital, Columbus, Ohio, USA
²¹Radiology, Stanford University, Stanford, California, USA
²²Biostatistics, University of Washington, Seattle, Washington, USA
²³Department of Biostatistics, University of Washington, Seattle, Washington, USA
²⁴Pediatrics, Division of Neonatology, University of Washington, Seattle, Washington, USA
²⁵Neurology, University of California San Francisco, San Francisco, California, USA
²⁶Radiology, St. Louis Children's Hospital and Washington University, Saint Louis, Missouri, USA

Acknowledgements We acknowledge the Clinical Coordinating Center (Yvonne Wu, Sandra Juul, Dennis Mayock, Fernando Gonzalez, Amy Goodman, John Feltner, Stephanie Hauge, Samantha Nikirk, Kelleen Nelson), Data Coordinating Center (Patrick Heagerty, Bryan Comstock, Christopher Nefcy, Mark Konodi), Neuroimaging Committee (Robert McKinstry, Jessica Wisnowski, Stefan Bluml, Ashok Panigrahy, Amit Mathur, Yvonne Wu, Sandra Juul, Kelleen Nelson), Data Safety and Monitoring Committee (Ronnie Guillet, Robin Ohls, Janet Soul, Jody Ciolino, Renee Shellhaas), Independent Medical Monitor (Mike Schreiber) and all of the Clinical Coordinators and study personnel participating at each site.

Collaborators The HEAL Study Group: Kaashif Ahmed (Children's Hospital of San Antonio and Methodist Children's Hospital), Mariana Baserga (Primary Children's Hospital and the University of Utah Hospital), Ellen Bendel-Stenzel (Children's Hospitals and Clinics of Minnesota), Lina Chalack, (University of Texas Southwestern), Taeun Chang (Children's National Medical Center), John Flibotte (Children's Hospital of Philadelphia), Amy Goodman (UCSF Benioff Children's Hospital), Fernando Gonzalez (UCSF Benioff Children's Hospital), Andrea Lampland (Children's Hospitals and Clinics of Minnesota), Nathalie Maitre (Nationwide Children's Hospital), Dennis Mayock (Seattle Children's Hospital and the University of Washington Medical Center), Ulrike Mietzsch (Riley Children's Hospital), Kelleen Nelson (UCSF Benioff Children's Hospital), Brenda Poindexter (Cincinnati Children's Hospital Medical Center), Rakesh Rao (Washington University Medical Center), David Riley (Cook Children's Hospital), Gregory M. Sokol (Riley Children's Hospital), Krisa Van Meurs (Stanford University), Hendrik Weitkamp, (Vanderbilt University Medical Center), Tai-Wei Wu (Children's Hospital Los Angeles), and Toby Yanowitz (Children's Hospital of Pittsburgh of UPMC and the Magee Women's Hospital).

Contributors YWW and SJ conceived the study, wrote the funding application and are responsible for the conduct of all aspects of the study; JLW, SB, AP, AMM, BC, PJH, SJ, YWW and RCM designed the neuroimaging protocol and oversee neuroimaging data collection and analysis; JB, P-SKC, JD, TF, SF, SDF, HWH, CYH, BK-F, MO, RP, SP, YMR, JRa, NR, JRu, DWS, MS, JT, SV, AV, MTW, DX and KY provided data and critical feedback on the neuroimaging protocol; JLW wrote the first draft of this manuscript; and, all authors contributed to manuscript revision and approved the final version for submission.

Funding This work was supported by grants from the National Institutes of Health (U01NS092764, U01NS092553 and K23HD099309).

Disclaimer The funding agency has no role in the design of the study, collection, management, analysis and interpretation of the data, the writing of the report and the decision to submit the report for publication.

Competing interests None declared.

Patient consent for publication Not required.

Provenance and peer review Not commissioned; externally peer reviewed.

Supplemental material This content has been supplied by the author(s). It has not been vetted by BMJ Publishing Group Limited (BMJ) and may not have been

peer-reviewed. Any opinions or recommendations discussed are solely those of the author(s) and are not endorsed by BMJ. BMJ disclaims all liability and responsibility arising from any reliance placed on the content. Where the content includes any translated material, BMJ does not warrant the accuracy and reliability of the translations (including but not limited to local regulations, clinical guidelines, terminology, drug names and drug dosages), and is not responsible for any error and/or omissions arising from translation and adaptation or otherwise.

Open access This is an open access article distributed in accordance with the Creative Commons Attribution Non Commercial (CC BY-NC 4.0) license, which permits others to distribute, remix, adapt, build upon this work non-commercially, and license their derivative works on different terms, provided the original work is properly cited, appropriate credit is given, any changes made indicated, and the use is non-commercial. See: <http://creativecommons.org/licenses/by-nc/4.0/>.

ORCID iD

Jessica L Wisnowski <http://orcid.org/0000-0002-4039-8362>

REFERENCES

- Lee ACC, Kozuki N, Blencowe H, *et al*. Intrapartum-related neonatal encephalopathy incidence and impairment at regional and global levels for 2010 with trends from 1990. *Pediatr Res* 2013;74:50–72.
- Edwards AD, Brocklehurst P, Gunn AJ, *et al*. Neurological outcomes at 18 months of age after moderate hypothermia for perinatal hypoxic ischaemic encephalopathy: synthesis and meta-analysis of trial data. *BMJ* 2010;340:c363.
- Jacobs SE, Berg M, Hunt R. Cooling for newborns with hypoxic ischaemic encephalopathy. *Cochrane Database Syst Rev Art* 2013:3–5.
- Juul SE, Comstock BA, Heagerty PJ, *et al*. High-Dose erythropoietin for asphyxia and encephalopathy (heal): a randomized controlled trial – background, aims, and study protocol. *Neonatology* 2018;113:331–8.
- Juul SE, Pet GC. Erythropoietin and neonatal neuroprotection. *Clin Perinatol* 2015;42:469–81.
- Wu YW, Bauer LA, Ballard RA, *et al*. Erythropoietin for neuroprotection in neonatal encephalopathy: safety and pharmacokinetics. *Pediatrics* 2012;130:683–91.
- Wu YW, Mathur AM, Chang T, *et al*. High-Dose erythropoietin and hypothermia for hypoxic-ischemic encephalopathy: a phase II trial. *Pediatrics* 2016;137.
- Rogers EE, Bonifacio SL, Glass HC, *et al*. Erythropoietin and hypothermia for hypoxic-ischemic encephalopathy. *Pediatr Neurol* 2014;51:657–62.
- Malla RR, Asimi R, Teli MA, *et al*. Erythropoietin monotherapy in perinatal asphyxia with moderate to severe encephalopathy: a randomized placebo-controlled trial. *J Perinatol* 2017;37:596–601.
- RANCK JB, WINDLE WF. Brain damage in the monkey, macaca mulatta, by asphyxia neonatorum. *Exp Neurol* 1959;1:130–54.
- Myers RE. Two patterns of perinatal brain damage and their conditions of occurrence. *Am J Obstet Gynecol* 1972;112:246–76.
- Myers RE. Four patterns of perinatal brain damage and their conditions of occurrence in primates. *Adv Neurol* 1975;10:223–34 <http://europepmc.org/abstract/MED/238372>
- Jacobson Misbe EN, Richards TL, McPherson RJ, *et al*. Perinatal asphyxia in a nonhuman primate model. *Dev Neurosci* 2011;33:210–21.
- McAdams RM, McPherson RJ, Kapur RP, *et al*. Focal brain injury associated with a model of severe hypoxic-ischemic encephalopathy in nonhuman primates. *Dev Neurosci* 2017;39:107–23.
- de Vries LS, Groenendaal F. Patterns of neonatal hypoxic-ischaemic brain injury. *Neuroradiology* 2010;52:555–66.
- Shankaran S, Barnes PD, Hintz SR, *et al*. Brain injury following trial of hypothermia for neonatal hypoxic-ischaemic encephalopathy. *Arch Dis Child Fetal Neonatal Ed* 2012;97:398–405.
- Rutherford M, Ramenghi LA, Edwards AD, *et al*. Assessment of brain tissue injury after moderate hypothermia in neonates with hypoxic-ischaemic encephalopathy: a nested substudy of a randomised controlled trial. *Lancet Neurol* 2010;9:39–45.
- Bashir RA, Vayalthirikkovil S, Espinoza L, *et al*. Prevalence and characteristics of intracranial hemorrhages in neonates with hypoxic ischaemic encephalopathy. *Am J Perinatol* 2018;35:676–81.
- Gorelik N, Faingold R, Daneman A, *et al*. Intraventricular hemorrhage in term neonates with hypoxic-ischemic encephalopathy: a comparison study between neonates treated with and without hypothermia. *Quant Imaging Med Surg* 2016;6:504–9.

- 20 Weeke LC, Groenendaal F, Mudigonda K, *et al.* A novel magnetic resonance imaging score predicts neurodevelopmental outcome after perinatal asphyxia and therapeutic hypothermia. *J Pediatr* 2018;192:33–40.
- 21 Sarkar S, Donn SM, Bapuraj JR, *et al.* The relationship between clinically identifiable intrapartum sentinel events and short-term outcome after therapeutic hypothermia. *J Pediatr* 2011;159:726–30.
- 22 Shankaran S, Laptook AR, McDonald SA, *et al.* Acute perinatal sentinel events, neonatal brain injury pattern, and outcome of infants undergoing a trial of hypothermia for neonatal hypoxic-ischemic encephalopathy. *J Pediatr* 2017;180:275–8.
- 23 Bonifacio SL, Glass HC, Vanderpluym J, *et al.* Perinatal events and early magnetic resonance imaging in therapeutic hypothermia. *J Pediatr* 2011;158:360–5.
- 24 Nasielli J, Papadogiannakis N, Löf E, *et al.* Hypoxic ischemic encephalopathy in newborns linked to placental and umbilical cord abnormalities. *J Matern Fetal Neonatal Med* 2016;29:721–6.
- 25 Vik T, Redline R, Nelson KB, *et al.* The placenta in neonatal encephalopathy: a case-control study. *J Pediatr* 2018;202:77–85.
- 26 Bingham A, Gundogan F, Rand K, *et al.* Placental findings among newborns with hypoxic ischemic encephalopathy. *J Perinatol* 2019;39:563–70.
- 27 Harteman JC, Nikkels PGJ, Benders MJNL, *et al.* Placental pathology in full-term infants with hypoxic-ischemic neonatal encephalopathy and association with magnetic resonance imaging pattern of brain injury. *J Pediatr* 2013;163:968–75.
- 28 Lachapelle J, Chen M, Oskoui M, *et al.* Placental pathology in asphyxiated newborns treated with therapeutic hypothermia. *J Neonatal Perinatal Med* 2015;8:33–40.
- 29 Mir IN, Johnson-Welch SF, Nelson DB. Placental pathology is associated with severity of neonatal encephalopathy and adverse developmental outcomes following hypothermia presented in poster format at the annual meeting of the pediatric academic societies, Vancouver, British Columbia, Canada. *Am J Obstet Gynecol* 2015;213:849.e1–7.
- 30 Frank CMC, Nikkels PGJ, Harteman JC, *et al.* Placental pathology and outcome after perinatal asphyxia and therapeutic hypothermia. *J Perinatol* 2016;36:977–84.
- 31 McKinstry RC, Miller JH, Snyder AZ, *et al.* A prospective, longitudinal diffusion tensor imaging study of brain injury in newborns. *Neurology* 2002;59:824–33.
- 32 Barkovich AJ, Miller SP, Bartha A, *et al.* MR imaging, MR spectroscopy, and diffusion tensor imaging of sequential studies in neonates with encephalopathy. *AJNR Am J Neuroradiol* 2006;27:533–47.
- 33 Kim HJ, Choi CG, Lee DH. High-b-Value diffusion-weighted MR imaging of hyperacute ischemic stroke at 1.5T. *Am J Neuroradiol* 2005;26:208 LP–15.
- 34 Cihangiroglu M, Citci B, Kilickesmez O, *et al.* The utility of high b-value DWI in evaluation of ischemic stroke at 3T. *Eur J Radiol* 2011;78:75–81.
- 35 Bednarek N, Mathur A, Inder T, *et al.* Impact of therapeutic hypothermia on MRI diffusion changes in neonatal encephalopathy. *Neurology* 2012;78:1420–7.
- 36 TW W, Tamrazi B, Hsu KH. Cerebral lactate concentration in neonatal hypoxic-ischemic encephalopathy: in relation to time, characteristic of injury, and serum lactate concentration. *Front Neurol* 2018;9:1–8.
- 37 Robertson NJ, Thayil S, Cady EB, *et al.* Magnetic resonance spectroscopy biomarkers in term perinatal asphyxial encephalopathy: from neuropathological correlates to future clinical applications. *Curr Pediatr Rev* 2014;10:37–47.
- 38 Alderliesten T, de Vries LS, Benders MJNL, *et al.* MR imaging and outcome of term neonates with perinatal asphyxia: value of diffusion-weighted MR imaging and ¹H MR spectroscopy. *Radiology* 2011;261:235–42.
- 39 Lally PJ, Montaldo P, Oliveira V, *et al.* Magnetic resonance spectroscopy assessment of brain injury after moderate hypothermia in neonatal encephalopathy: a prospective multicentre cohort study. *Lancet Neurol* 2019;18:1–11.
- 40 Hope PL, Costello AM, Cady EB, *et al.* Cerebral energy metabolism studied with phosphorus NMR spectroscopy in normal and birth-asphyxiated infants. *Lancet* 1984;2:366–70.
- 41 Amess PN, Penrice J, Wylezinska M, *et al.* Early brain proton magnetic resonance spectroscopy and neonatal neurology related to neurodevelopmental outcome at 1 year in term infants after presumed hypoxic-ischaemic brain injury. *Dev Med Child Neurol* 1999;41:436–45.
- 42 Robertson NJ, Lewis RH, Cowan FM, *et al.* Early increases in brain myo-inositol measured by proton magnetic resonance spectroscopy in term infants with neonatal encephalopathy. *Pediatr Res* 2001;50:692–700.
- 43 Wisnowski JL, Wu T-W, Reitman AJ, *et al.* The effects of therapeutic hypothermia on cerebral metabolism in neonates with hypoxic-ischemic encephalopathy: An in vivo ¹H-MR spectroscopy study. *J Cereb Blood Flow Metab* 2016;36:1075–86.
- 44 Gano D, Chau V, Poskitt KJ, *et al.* Evolution of pattern of injury and quantitative MRI on days 1 and 3 in term newborns with hypoxic-ischemic encephalopathy. *Pediatr Res* 2013;74:82–7.
- 45 Barkovich AJ, Hajnal BL, Vigneron D, *et al.* Prediction of neuromotor outcome in perinatal asphyxia: evaluation of Mr scoring systems. *AJNR Am J Neuroradiol* 1998;19:143–9.
- 46 Rutherford MA, Pennock JM, Counsell SJ, *et al.* Abnormal magnetic resonance signal in the internal capsule predicts poor neurodevelopmental outcome in infants with hypoxic-ischemic encephalopathy. *Pediatrics* 1998;102:323–8.
- 47 Cheong JLY, Coleman L, Hunt RW, *et al.* Prognostic utility of magnetic resonance imaging in neonatal hypoxic-ischemic encephalopathy: substudy of a randomized trial. *Arch Pediatr Adolesc Med* 2012;166:634–40.
- 48 Trivedi SB, Vesoulis ZA, Rao R, *et al.* A validated clinical MRI injury scoring system in neonatal hypoxic-ischemic encephalopathy. *Pediatr Radiol* 2017;47:1491–9.
- 49 Goergen SK, Ang H, Wong F, *et al.* Early MRI in term infants with perinatal hypoxic-ischaemic brain injury: interobserver agreement and MRI predictors of outcome at 2 years. *Clin Radiol* 2014;69:72–81.
- 50 Rutherford M, Malamateniou C, McGuinness A, *et al.* Magnetic resonance imaging in hypoxic-ischaemic encephalopathy. *Early Hum Dev* 2010;86:351–60.
- 51 Thayil S, Chandrasekaran M, Taylor A, *et al.* Cerebral magnetic resonance biomarkers in neonatal encephalopathy: a meta-analysis. *Pediatrics* 2010;125:e382–95.
- 52 van Laerhoven H, de Haan TR, Offringa M, *et al.* Prognostic tests in term neonates with hypoxic-ischemic encephalopathy: a systematic review. *Pediatrics* 2013;131:88–98.
- 53 Alger JR. Quantitative proton magnetic resonance spectroscopy and spectroscopic imaging of the brain: a didactic review. *Top Magn Reson Imaging* 2010;21:115–28.
- 54 Lange T, Dydak U, Roberts TPL, *et al.* Pitfalls in lactate measurements at 3T. *AJNR Am J Neuroradiol* 2006;27:895 LP–901 <http://www.ajnr.org/content/27/4/895.abstract>
- 55 Endorsement SOF. Neonatal encephalopathy and neurologic outcome, second edition. *Pediatrics* 2014;133:e1482–8.
- 56 Barkovich AJ, Baranski K, Vigneron D, *et al.* Proton MR spectroscopy for the evaluation of brain injury in asphyxiated, term neonates. *AJNR Am J Neuroradiol* 1999;20:1399–405.
- 57 Alderliesten T, de Vries LS, Staats L, *et al.* MRI and spectroscopy in (near) term neonates with perinatal asphyxia and therapeutic hypothermia. *Arch Dis Child Fetal Neonatal Ed* 2017;102:F147–52.
- 58 Bonifacio SL, Saporta A, Glass HC, *et al.* Therapeutic hypothermia for neonatal encephalopathy results in improved microstructure and metabolism in the deep gray nuclei. *AJNR Am J Neuroradiol* 2012;33:2050–5.
- 59 Lally PJ, Pauliah S, Montaldo P, *et al.* Magnetic resonance biomarkers in neonatal encephalopathy (marble): a prospective multicountry study. *BMJ Open* 2015;5:e008912.
- 60 Azzopardi D, Robertson NJ, Bainbridge A, *et al.* Moderate hypothermia within 6 H of birth plus inhaled xenon versus moderate hypothermia alone after birth asphyxia (TOBY-Xe): a proof-of-concept, open-label, randomised controlled trial. *Lancet Neurol* 2016;15:145–53.
- 61 Thayil S, Oliveira V, Lally PJ, *et al.* Hypothermia for encephalopathy in low and middle-income countries (HELIX): study protocol for a randomised controlled trial. *Trials* 2017;18:432.
- 62 Ancora G, Testa C, Grandi S, *et al.* Prognostic value of brain proton MR spectroscopy and diffusion tensor imaging in newborns with hypoxic-ischemic encephalopathy treated by brain cooling. *Neuroradiology* 2013;55:1017–25.
- 63 Sijens PE, Wischniowsky K, Ter Horst HJ. The prognostic value of proton magnetic resonance spectroscopy in term newborns treated with therapeutic hypothermia following asphyxia. *Magn Reson Imaging* 2017;42:82–7.
- 64 Mitra S, Kendall GS, Bainbridge A, *et al.* Proton magnetic resonance spectroscopy lactate/N-acetylaspartate within 2 weeks of birth accurately predicts 2-year motor, cognitive and language outcomes in neonatal encephalopathy after therapeutic hypothermia. *Arch Dis Child Fetal Neonatal Ed* 2019;104:F424 LP–32.
- 65 Chan AW, Tetzlaff JM, Altman DG. Spirit 2013 statement: defining standard protocol items for clinical trials. *Chinese J Evidence-Based Med* 2013;13:1501–7.
- 66 Mellon RD, Simone AF, Rappaport BA. Use of anesthetic agents in neonates and young children. *Anesth Analg* 2007;104:509–20.

- 67 Nakagawa S, Johnson PCD, Schielzeth H. The coefficient of determination R^2 and intra-class correlation coefficient from generalized linear mixed-effects models revisited and expanded. *J R Soc Interface* 2017;14::20170213
- 68 Müller R, Büttner P. A critical discussion of intraclass correlation coefficients. *Stat Med* 1994;13:2465–76.
- 69 Blüml S, Wisnowski JL, Nelson MD, *et al.* Metabolic maturation of white matter is altered in preterm infants. *PLoS One* 2014;9:e85829.
- 70 Baguley T. Understanding statistical power in the context of applied research. *Appl Ergon* 2004;35:73–80.
- 71 Malyarenko D, Galbán CJ, Londy FJ, *et al.* Multi-system repeatability and reproducibility of apparent diffusion coefficient measurement using an ice-water phantom. *J Magn Reson Imaging* 2013;37:1238–46.
- 72 Fortin J-P, Parker D, Tunç B, *et al.* Harmonization of multi-site diffusion tensor imaging data. *Neuroimage* 2017;161:149–70.